

## SPADE: A rock-crushing and sample-handling system developed for Mars missions

Candice J. Hansen,<sup>1</sup> David A. Paige,<sup>2</sup> Gregory Bearman,<sup>1</sup> Stephen Fuerstenau,<sup>1\*</sup> Jennifer Horn,<sup>1</sup> Colin Mahoney,<sup>1</sup> Steven Patrick,<sup>1</sup> Greg Peters,<sup>1</sup> Josh Scherbenski,<sup>1</sup> Lori Shiraishi,<sup>1</sup> and Wayne Zimmerman<sup>1</sup>

Received 3 February 2005; revised 30 June 2006; accepted 26 February 2007; published 21 June 2007.

[1] A novel system has been developed to access and analyze the interior of rocks on Mars by crushing rocks. A miniature rock crusher has been prototyped along with a method for distribution of the fines and fragments produced by the rock crusher to inspection and analysis instruments. The science goals and advantages of this approach are substantial with respect to understanding the geologic and climate history of Mars via the investigation of its mineralogy and petrology. The system is described in detail, and results of various performance metrics are reported. Engineering considerations, constraints on functionality, fault tolerance, and its previously-planned deployment on the 2009 Mars Science Laboratory mission are described.

**Citation:** Hansen, C. J., et al. (2007), SPADE: A rock-crushing and sample-handling system developed for Mars missions, *J. Geophys. Res.*, 112, E06008, doi:10.1029/2005JE002413.

### 1. Introduction

[2] Access to the interior of rocks on Mars is essential for understanding Mars' petrology, mineralogy, and geologic history. The spectral signature of the potentially diverse mineralogy of rocks on Mars is veiled by ubiquitous dust and may be further hidden by the weathered rind on surface rocks. We have developed a rock crusher and a sample distribution system under the auspices of NASA's Planetary Instrument Design and Development Program (PIDDP), augmented with funding from the Mars Technology Program, designed to be part of the payload of a surface rover or lander. It's called "SPADE", the Sample Processing and Distribution Experiment. Its purpose is to access the interiors of rocks on Mars and prepare samples for analysis by a suite of in situ instruments.

[3] The system consists of a rock crusher which produces rock fragments and fines, a sample sorting system for separating fragments from fines, a sample wheel with bins for fragments and fines that moves the rock products to in situ instruments for inspection and analysis, and sweepers or trap doors for removing the products from the wheel (Figures 1–4). The rock crusher is based on a commercial "jaw crusher" design. There are no consumables that will limit the lifetime of the crusher and wheel.

[4] The field of rock comminution is well documented for commercial endeavors on Earth. This paper is not aimed at that field of experts but rather at the interests of the planetary

science community for SPADE's specific use on the surface of Mars. Rover missions, by design, explore field sites at a human scale. SPADE's scientific strategy is patterned after field methods that have been successfully employed by geologists on Earth. Access to the pristine interior of rocks on Mars' surface, past their dusty and weathered surfaces, is the first step for many diverse goals that can be contemplated for Mars surface missions, outlined in sections 2 and 3. Sections 4 and 5 describe SPADE's development history. The first deployment of SPADE could have been on the 2009 Mars Science Laboratory mission (MSL), described in section 5. Subsequent sections describe the performance of the system in detail with respect to metrics important to its eventual science users.

### 2. Science Motivation for SPADE

[5] The most perplexing paradox confronting Mars scientists today is the apparent conflict between mineralogical data and surface morphology data from orbiters with respect to whether liquid water existed on the surface of Mars for an extended length of time. Neutron spectrometer data returned from Odyssey offers overwhelming evidence for abundant water frozen in the subsurface at high latitudes [Boynton *et al.*, 2002], while Mariner 9, Viking, and Mars Global Surveyor (MGS) images indicate past modification of the surface by water (for example, numerous references in the works of Carr [1981], Parker *et al.*, 1993; Baker, 2001; Malin and Edgett, 2003). Near IR and thermal spectroscopy data, however, do not support the concept of extensive hydrous alteration of the surface, with the possible exception of the hematite site in Meridiani Planum [e.g., Christensen *et al.*, 2001, 2004]. Indeed, the presence of olivine argues directly against recent surface modification [Hoefen *et al.*, 2003]. This is one of the major puzzles confronting Mars

<sup>1</sup>Jet Propulsion Laboratory, California Institute of Technology, Pasadena, California, USA.

<sup>2</sup>Department of Earth and Space Sciences, University of California, Los Angeles, Los Angeles, California, USA.

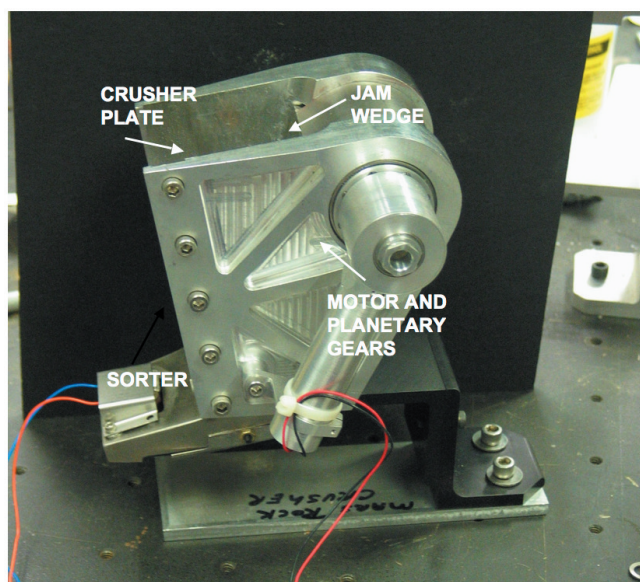


**Figure 1.** The Rockhound rock crusher is ~10 cm (4 in) tall. One cycle of the crusher plate takes 3.5 min. It requires a few hours to crush a rock (depending on the size and hardness of the rock). This prototype has crushed hundreds of rocks.

scientists today. To resolve this issue, one must be able to examine rocks and outcrops on the surface to accurately interpret data taken from orbit. The Mars Exploration Rovers (MER) have now proven the value of sending rovers to intriguing sites to directly investigate the geology and mineralogy [Squyres *et al.*, 2004a]. The use of the MER rock abrasion tool allowed the science team to remove surficial dust and thin patinas to determine the mineralogy of rocks at the Gusev Crater landing site [Bell *et al.*, 2004; Herkenhoff

*et al.*, 2004; Gellert *et al.*, 2004; Morris *et al.*, 2004; Christensen and Ruff, 2004] and the outcrop at the Meridiani Planum landing site [Squyres *et al.*, 2004b, 2004c]. By getting past the rock exterior and examining rocks at close range at these two sites, MER has begun to resolve the apparent conflict between different orbiter data sets. The scientific outcome, understanding Mars' climate history, is immense.

[6] The fundamental basis for understanding the Earth's geological and biological history comes from studying the record contained in its rocks. On Earth, there are a tremendous variety of rocks, each of which can be classified on the basis of three fundamental properties as follows: texture, mineralogy, and chemistry. Remote sensing studies, the Viking and Pathfinder landers, and the Mars Exploration Rovers have provided interesting clues to rock textures, mineralogy, and chemistry, but have not explored the full potential variety of Mars' rocks [McSween *et al.*, 1999, 2004]. For example, are the ancient highlands rocks coarse-grained gabbros or fine-grained basalts? Are they primary igneous rocks or are they sedimentary rocks formed in ancient lakes? The fact that, from orbit, everything looks so blandly similar spectrally is attributed to Mars' extensive eolian activity and the accompanying global distribution of dust [e.g., Johnson *et al.*, 2002; Bandfield *et al.*, 2000; Arvidson *et al.*, 1989; Christensen *et al.*, 2000; Mustard and Sunshine, 1995]. Interpretation of rock data from surface missions has also been hindered by the ubiquitous dust coating [Smith *et al.*, 1997; Bell *et al.*, 2000; Christensen *et al.*, 2004], until MER's use of the rock abrasion tool. Attempting to characterize rocks by simply observing their exterior surfaces is also challenged by the fact that gases and aerosols in the Martian atmosphere absorb and scatter solar radiation and emit infrared radiation [Smith *et al.*, 2000; Johnson *et al.*, 2002].

[7] A complete investigation of rocks involves studying both their exterior surfaces and their interiors. The exterior

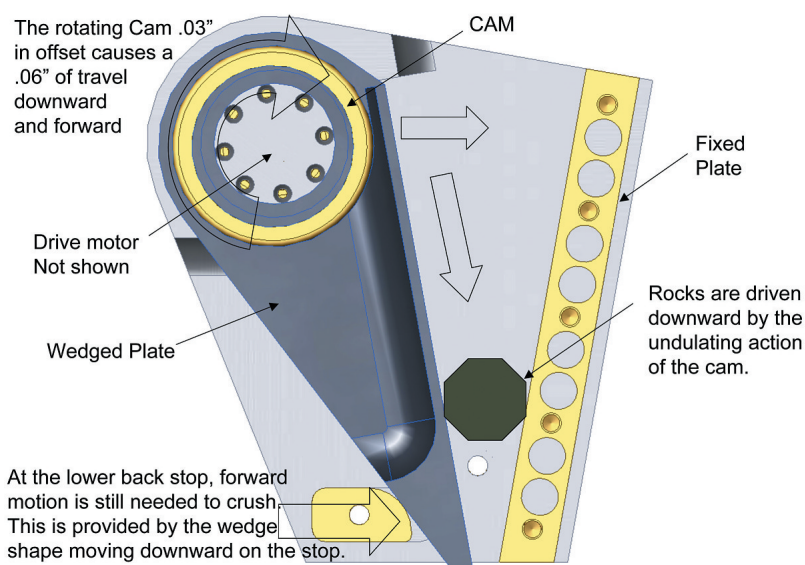


**Figure 2.** The rock crusher has a fixed plate and a moving plate which form a wedge. The moving plate rotates, forcing the rock down as it compresses. The separation between the plates at the top determines the size of the largest rock that can be dropped in the crusher. The width of the exit gap at the bottom constrains the size of the fragments that can fall through.





**Figure 3.** Crushed materials that are smaller than the smallest gap between the plate and the wedge fall into the sorter, which separates the materials into two size categories. The mechanical screening and vibrating process separates large fragments from fine particles causing them to fall into adjacent bins. Once either of the bins have reached peak capacity (coarse or fines, whichever is first), the sample-handling system autonomously shuts off the crusher and moves the sample wheel, placing an empty coarse bin and an empty fines bin under the sorter.

surface is exposed to a host of environmental processes which can significantly alter texture, mineralogy, and chemistry [Gooding *et al.*, 1992]. Physical and chemical weathering of rock surfaces may hinder examination of mineral fabrics and textures, and weathering rinds may have significantly different properties than those of the rock's interior. In addition, on the basis of the Viking lander Gas Chromatograph Mass Spectrometer (GCMS) results, the Martian surface environment is presently hostile to the preservation of organic material [Biemann *et al.*, 1977]. If organic material is preserved in Martian rocks, a strategy is required which allows access to and examination and characterization of rock interiors, as well as processing of the sample for its ingestion into in situ analysis instruments.

[8] SPADE will enable the in situ scientific investigations of Mars' rocks. With SPADE, one can

[9] • Access rock interiors;

[10] • Sort rock crusher products by size (fines, small fragments);

[11] • Distribute fines to in situ analysis instruments which require them, such as X-ray fluorescence spectrometers, evolved gas analyzers, or wet chemical analysis instruments;

[12] • Distribute rock fragments to a suite of instruments designed to analyze the mineralogy and texture of rocks by close-up viewing, such as microscopic imagers or spectrometers. The rock fragments produced by the rock crusher expose fresh surfaces. The fragments can be examined with a microscopic imager to inspect grain size, cleavage planes, and texture. Instruments such as evolved gas analyzers or X-ray fluorescence spectrometers require fines or powders,

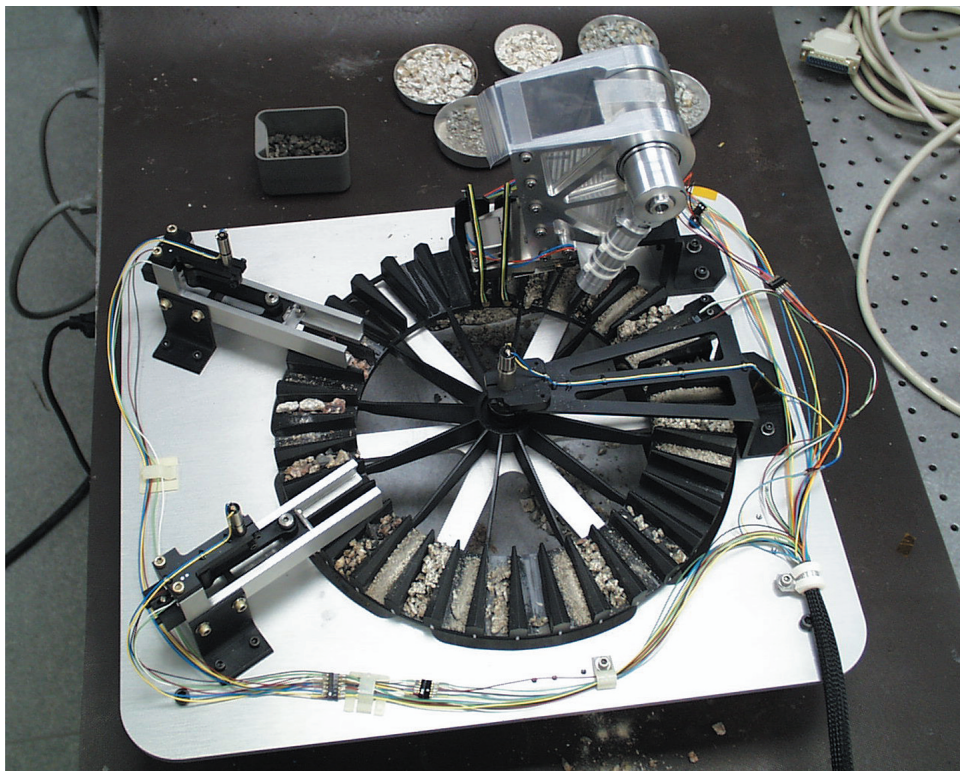


**Figure 4.** The complete original system featured the rock crusher, products sorted into small fragments and fines, the sample wheel for presentation of products to inspection instruments, and sweepers for moving product to in situ analysis instruments, cache, or discard to the ground.

produced readily by the crushing process. The instruments that can potentially make in situ measurements is a lengthy list, including, for example, microscopic imagers, three-dimensional imagers, near-IR spectrometers, alpha proton X-ray spectrometers, Mossbauer spectrometers, X-ray fluorescence spectrometers, chemistry experiments, organics detectors, differential scanning calorimetry, and evolved gas analyzers.

[13] Exposure of fresh rock faces is the first step in determining mineral fabrics and textures to classify a rock and to estimate mineralogy, origin, and history. For example, in igneous rocks, grain size is indicative of the pressure and temperature of magmatic processes and enables reconstruction of the crystallization history. Porosity contains clues to the volatility of the magma. Evidence of quenching or sudden pressure release is contained in the identity of the rock. Since SPADE produces a well-graded spectrum of particle sizes, the larger fragments can be separated and sent to optical instruments for petrographic analysis. Grains up to the size of the plate separation are unharmed by the crushing process, and even larger crystals may be preserved if longer slivers slide through the long dimension of the crusher.

### 3. SPADE Development History

[14] Development of the SPADE system began in 1997 as part of a proposal effort called “Rockhound,” responding to the ‘01 Announcement of Opportunity for a small rover payload [Hansen *et al.*, 1997]. As proof of concept the Rockhound team built a prototype miniature rock crusher. It is worth noting that this prototype crusher is still being used and has crushed hundreds of rocks in the course of our years of investigation of rock crusher performance. Subsequent development was supported first by PIDDP then augmented by the Mars Technology Program. The development of SPADE’s prototype hardware for the sample sorting and distribution system (to work with the prototype rock crusher), as well as further characterization of rock crusher performance, was funded by the PIDDP program in 2001 [Hansen *et al.*, 2001]. We designed, fabricated, and tested the sample sorter, sample wheel, “bin-full” LED detectors, and sample sweepers, running with the rock crusher. An extensive test program involved crushing a large number of rocks to seek out the limits of this approach and analyze rock crusher performance. The PIDDP team carried out an end-to-end systems analysis approach that culminated in the acquisition of representative types of science data. In 2002 the SPADE Principal Investigator (Candice Hansen) brought the rock crusher and sample-handling system to the attention of the management of the Mars Science Laboratory (MSL) rover planned for the 2009 Mars launch opportunity. In order to leverage the technology development aimed at the 2009 mission, more funding was allocated by the Mars Technology Program to SPADE. The additional funding was directed to the mitigation of sample cross contamination, a complete mechanical and finite element analysis to produce a lighter second generation of rock crushers, and prototyping of a rock release mechanism. In 2003 the MSL project decided to incorporate SPADE in its rover design. The ability to crush rocks and produce fines for analysis by in situ instruments became part of the rover capability advertised in the 2004 Announcement of Opportunity. A payload of instruments

was selected in December 2004 (see section 6). Modification of SPADE to meet the specific needs of the MSL project is ongoing.

## 4. SPADE Detailed Description

[15] SPADE has progressed and changed, due to lessons learned in the development process, from the originally conceived design. The sample delivery system in particular has evolved. Both are described below as the evolution is instructive.

### 4.1. Original Design

[16] The original SPADE system consisted of a rock crusher which crushes small rocks, a sample sorter which separates coarse fragments from fines, a sample wheel which positions rock fragments and fines for viewing, and sample sweepers which dispense selected fine or rock fragments into analysis instruments or sample cache and discard the rest.

#### 4.1.1. Rock Crusher

[17] The rock crusher, shown in Figure 1, has two plates with hardened stainless steel surfaces supported by parallel sidewalls. One plate is “fixed” and is integral to the crusher support structure. As illustrated in Figure 2 the other plate moves both horizontally and vertically with respect to the opposing plate via a cam mounted to its rear surface. This rectangular plate is constrained by the cam at the top and by a backing cam and spring at the bottom and forms a 20° wedge to the fixed plate. During operation, the drive cam moves the plate both inward and downward (simultaneously) during the crushing stroke and upward and backward during the return stroke. The compression stroke applies the crushing force while the downward motion drives the rock further into the wedge formed by the two plates. The rock fractures along its weakest joints. As smaller fragments are created by the fracturing of the rock they fall lower in the crusher and, when small enough, exit the crusher. The maximum width of rock fragments that can fall through the crusher to the sample sorter is determined by the base separation of the crushing plates, which is 0.5 cm in the Rockhound prototype crusher. Note that the crusher can produce fragments with large aspect ratios if the long dimension of a fragment happens to align with the exit plate axis.

[18] The crusher is driven with a high-speed motor (~18,000 RPM) that is geared down twice, first by a reduction gear and then by a planetary gear attached to the cam that drives the wedge. With the present gearing, the cam plus wedge system complete a revolution in ~3.5 min, for a total reduction of ~60,000:1. The final prototype crusher configuration has an offset of 0.75 mm (0.03 in.) in the drive cam. The drive motor and gearbox delivers 28.25 N-m (250 lb-in.) of torque. Force produced by the cam at the top of the wedge is 37,000 N (250 lb-in./0.03 in. = 8,333 lb). Hardened steel was chosen for the plates to minimize plate surface scrapings being mixed with the rock itself. Later prototypes have used titanium to reduce mass.

[19] The separation of the plates at the top of the crusher limits the size of the largest rock that can be introduced into the crusher. The size of the system can be scaled up or down to meet the science requirements of the mission and volume and mass constraints. The separation of the plates at the



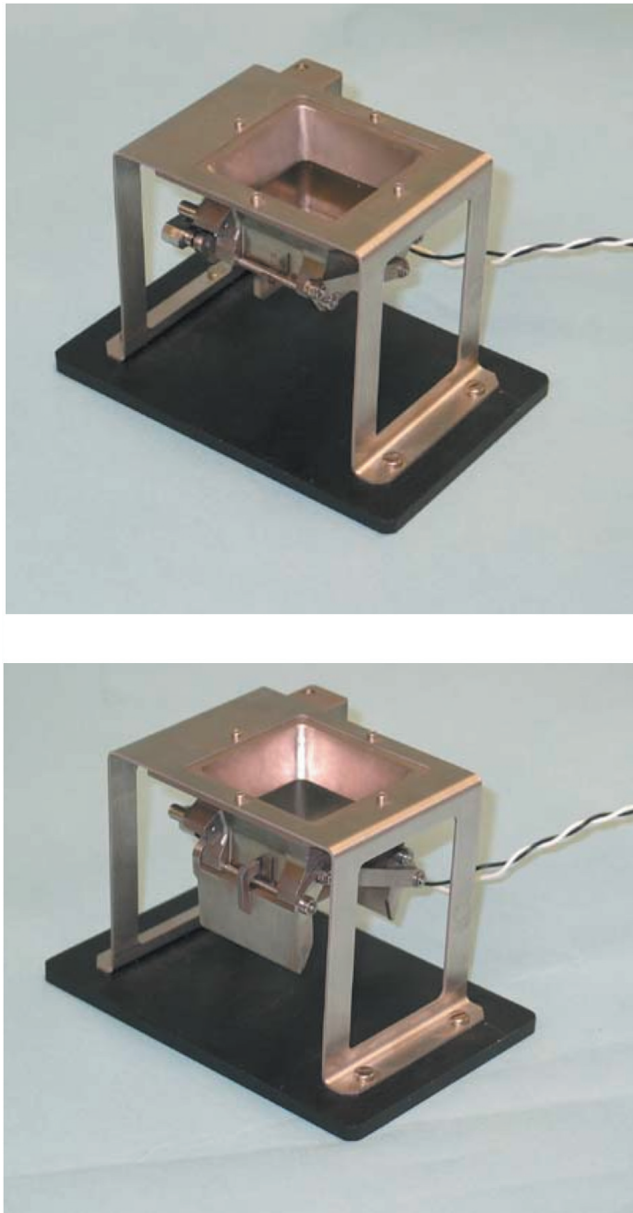


**Figure 5.** The trap door configuration is shown with the doors closed (top image) and open (bottom image).

bottom determines the largest fragment size. Plate separation at the bottom of the crusher is selectable at the time of final fabrication. We have experimented with a variety of plate separations to investigate the fraction of fines versus fragments produced as a function of plate separation at the exit. Results are described below in section 7.

#### 4.1.2. Sample Sorter

[20] The crusher action produces fines and small pieces in addition to the largest fragment size, shown in Figure 3. The crushed material is sorted into two selectable size ranges. For the prototype system, fines  $< 2$  mm were separated from coarse fragments  $> 2$  mm. The sorting device is a ramp with a 2-mm sifting grate above one sample bin and a larger exit area above the adjacent sample bin. As particles are deposited onto an angled ramp, an electromagnetic vibration generator assists the particles' motion down the ramp. As the smaller

particles filter through the sifting grate, the larger particles continue toward the end of the ramp and fall onto the wheel (see Figures 2 and 5). The fine size sorted out is selectable and will likely end up smaller than 2 mm for the MSL application.

#### 4.1.3. Sample Wheel

[21] The sample wheel is a light-weight anodized aluminum circular table, driven in the center by an actuator with a shaft encoder. The wheel rotates in the horizontal plane and moves the rock crusher products to predetermined stops. An LED/photodiode system shines an optical beam across the sample bins. The crusher operates until the beam is broken. At that time, the crusher and sorter will stop momentarily and the sample wheel indexes to the next position. One can envision a series of inspection instruments such as microscopic imagers and spectrometers mounted above the sample wheel to acquire data of the crushed rock products.

#### 4.1.4. Sample Sweeper

[22] The Sample Sweeper is designed to rake across the sample wheel. A simple push/pull motion is suitable for moving the sample material out of the bin. Once data has been returned to Earth from the inspection instruments several options are conceivable as follows: A sample can undergo further analysis, a sample can be cached for future retrieval, or a sample can be discarded. The sample being discarded is simply pushed off onto the ground. To deliver a sample to the next suite of instruments or cache, a gravity feed is envisioned. This step is very dependent on the nature of the sample recipient and will be determined by the mission application. The lower force of gravity on Mars will also drive design requirements such as slopes of sorters and funnels.

[23] As shown in Figure 4 the entire system has been prototyped and tested extensively.

### 4.2. Current SPADE Design, Modified Because of Test Results and MSL Requirements

#### 4.2.1. Sample Bin With Trap Door

[24] During the test program, there was a serious tendency for rocks to get lodged between the sample bins and sorter and sides. Cross contamination and cleaning of sample bins were also concerns. Fragments had a tendency to skip into fine sample bins. The final blow to the sample bin/sweeper design was the MSL requirement for operation at an angle of up to  $20^\circ$ . This led to a new design for the sample bin that features an enclosed bin with trap doors at the bottom, shown in Figure 5. The bin doors are opened with an over the center knee that is actuated by a solenoid. As mass (sample) is added on top of the doors, it keeps them closed, like the proverbial Chinese finger lock.

[25] The opening of the trap door occurs with a bang, dislodging the contents effectively, thus minimizing cross contamination, as discussed in section 7. A carousel with bins with trap doors has essentially the same functionality that the sample wheel with sweepers offered and is more robust in a remote setting. A prototype carousel with bins has not yet been built but the expectation is that only minor modifications to the LED control and sorter will be necessary. The bin design has been tested for shock and vibration at MSL required levels.

#### 4.2.2. Snake Jaw Rock Release

[26] There are times when it is desirable to release a rock from the crusher before the crushing process has finished. This functionality is described in section 9.

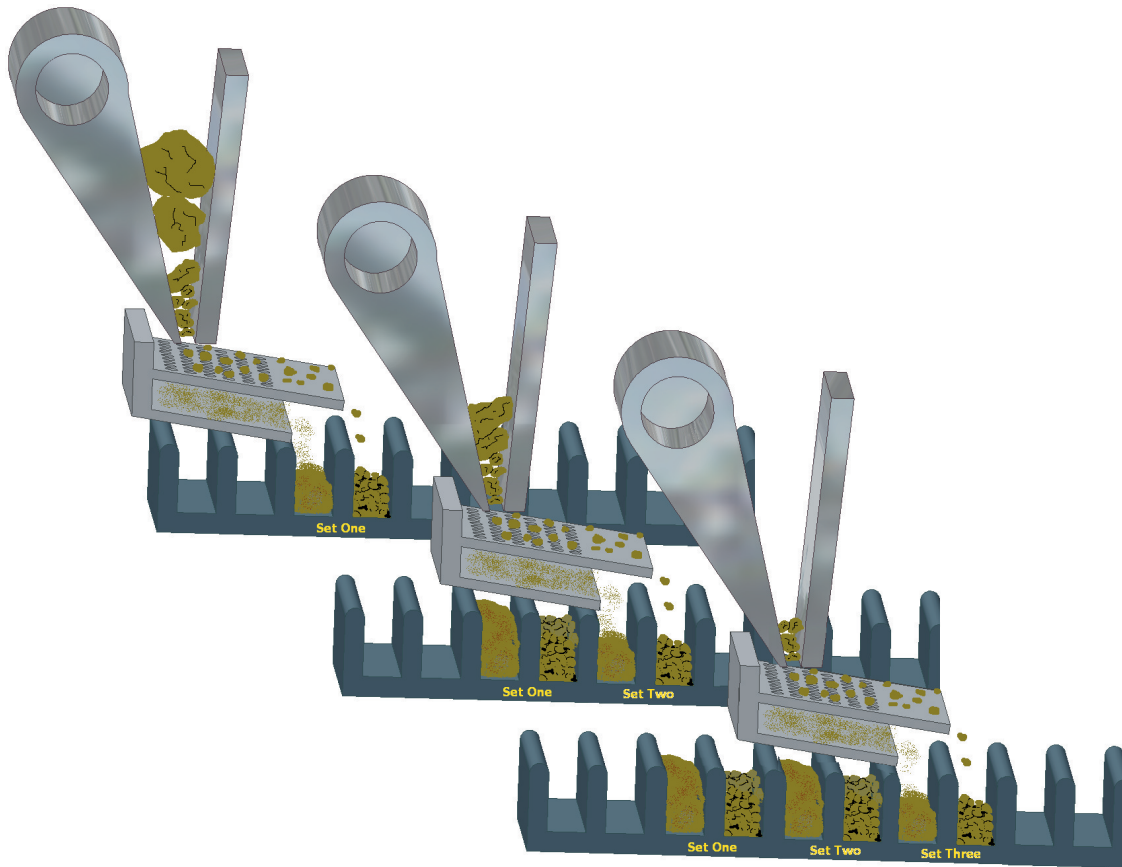


**Figure 6.** SPADE sequence of operation is illustrated. Rock crusher operation, sorter operation, and sample wheel positioning are orchestrated autonomously.

#### 4.3. Operation and Control of the SPADE System

[27] The sequence starts with the introduction of a rock into the crusher. Since the size of a rock to be crushed is limited by the separation of the crusher walls at the top, the opening of the rock crusher will require a mask to prevent the introduction of a rock that is too big and could get stuck. In actual use on Mars a rock will be imaged prior to introduction into the crusher for initial characterization.

[28] The rotary action of the crusher walls cracks the rock and works the pieces down further into the crusher. The

rock crusher continuously crushes rocks onto the sample sorter as long as the sample wheel (or carousel) is not commanded to move. If the sample wheel is commanded to move, the rock crusher operation is stopped until the sample wheel stops moving. Engineering data from the crusher motor currents will be used to detect when a rock has been completely crushed and when the crusher is empty.

[29] The sample wheel motion may be commanded either automatically or manually. In optical automatic mode, the sample wheel is commanded to move by the optical sensors at

**Table 1.** Mineral and Rock Types Crushed

Mineral/Rock	Name	Formula	Mohs Hardness of Mineral	Specific Gravity
Gypsum (Mineral)	Hydrated Calcium Sulfate	$\text{CaSO}_4 \cdot 2(\text{H}_2\text{O})$	2	2.3
Forsterite (Mineral)	Magnesium silicate	$(\text{Mg, Fe})_2\text{SiO}_4$	6.5–7	3.2
Feldspar (Mineral)	Sodium aluminum silicate	$\text{NaAlSi}_3\text{O}_8$		2.61
Anorthite (Mineral)	Calcium aluminum silicate	$\text{CaAl}_2\text{Si}_2\text{O}_8$		2.76
Diopside (Mineral)	Calcium magnesium silicate	$\text{CaMgSi}_2\text{O}_6$	5–6	3.3
Calcite (Mineral)	Calcium carbonate	$\text{CaCO}_3$	3	2.7
Andesite (Rock)	Sodium calcium aluminum silicate	$\text{Na}(70\text{--}50\%) \text{Ca}(30\text{--}50\%) (\text{Al, Si})\text{AlSi}_2\text{O}_8$		2.68–2.71
Dolomite (Mineral)	Calcium magnesium carbonate	$\text{CaMg}(\text{CO}_3)_2$	3.54	2.86
Hematite (Mineral)	Iron oxide	$\text{Fe}_2\text{O}_3$	5–6	5.3
Serpentine (Mineral)	Magnesium iron silicate hydroxide	$(\text{Mg, Fe})_3\text{Si}_2\text{O}_5(\text{OH})_4$	3–4.5	2.2–2.6
Magnetite (Mineral)	Iron oxide	$\text{Fe}_3\text{O}_4$	5.5–6.5	5.1
Siderite (Mineral)	Iron carbonate	$\text{FeCO}_3$	3.5–4.5	3.9+
Augite (Mineral)	Calcium sodium magnesium iron aluminum silicate	$(\text{Ca, Na})(\text{Mg, Fe, Al})(\text{Al, Si})_2\text{O}_6$	5–6	3.2–3.6
Sandstone (Rock)	Medium-grained sedimentary sandstone			
Olivine Basalt (Rock)	Magnesium-iron silicate, in basalt			

**Table 2.** Exit Gap Configurations Tested

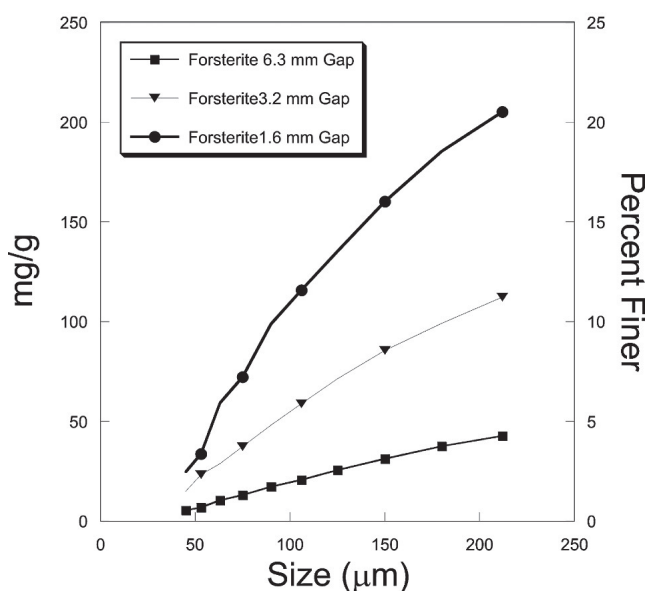
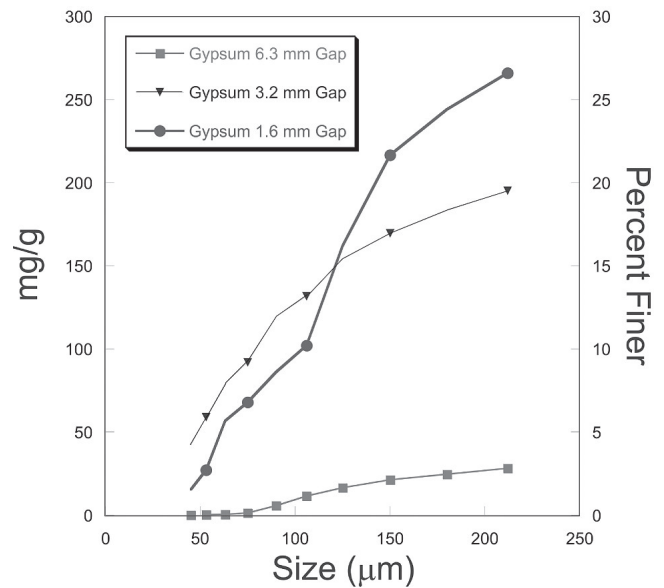
Stationary Plate Configuration	Exit Gap in Inches (in.)	Exit Gap in Millimeters (mm)
Setting “P1”	0.25	6.3
Setting “P3”	0.125	3.2
Setting “P2”	0.0625	1.6

the two bins being filled by the crusher/sorter. The optical sensors look across each of the bins to determine if the bin is full. Since rocks falling into the bin pass through the beam, the optical sensor must indicate that the beam is blocked for 1.5 s continuously in order to provide an indication that the bin is full. Dust on the optics may attenuate the signal, but a full bin is still detectable. When either of the two bins is indicated as full, crusher and sorting operations are stopped, the sample wheel is rotated until the next two bins are positioned under the crusher/sorter, and crusher/sorter operation is resumed, as illustrated in Figure 6.

[30] The fines and fragments in the sample wheel (or carousel) are rotated to inspection instruments for close-up examination. The trap doors are opened over an analysis instrument’s entry port to deliver fines (which may include a second sort of fine material to go to a smaller size range) or opened over the ground to empty samples for which no further analysis is desired.

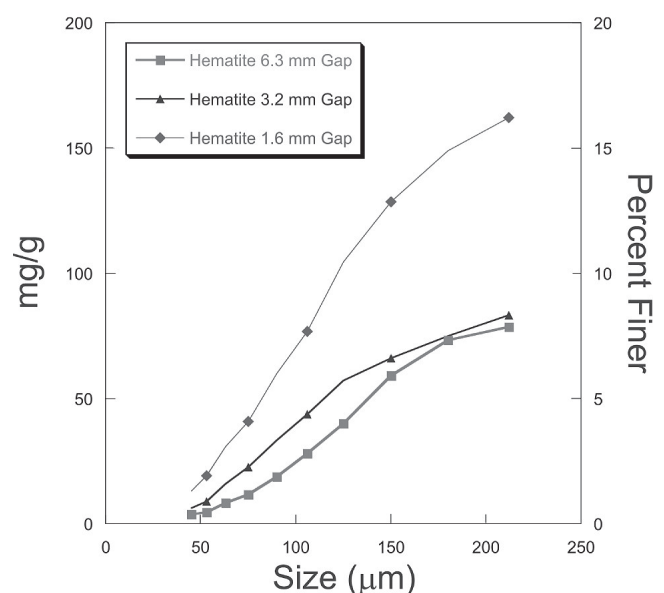
## 5. SPADE Deployment on MSL

[31] The overall science objective of the MSL mission is to explore and quantitatively assess a local region on the Mars surface as a potential habitat for life, past or present. MSL will examine Martian rocks and soils to determine the geologic processes that formed them, study the Martian atmosphere, and determine the distribution and circulation of water and carbon dioxide.

**Figure 7.** The fraction of fines passing through each sieve for three different exit plate openings is shown for forsterite.**Figure 8.** The fraction of fines passing through each sieve for three different exit plate openings is shown for gypsum.

[32] The instruments selected for the MSL mission are grouped as mast-mounted “remote sensing,” arm-mounted “contact instruments,” and the “analytical laboratory” suite. SPADE could interface to the analytical laboratory instruments and the arm-mounted microscopic imager (MAHLI, Mars Hand Lens Imager). MAHLI will be used to image the rock fragments, with resolution 2.4 times better than the microscopic imager carried by the 2003 Mars Exploration Rovers. The crushing operation may be interrupted to allow MAHLI to image the interior surfaces of the rocks exposed in the crushing process.

[33] Most SPADE requirements would come from the two analytical laboratory instruments. “CheMin” is an X-ray

**Figure 9.** The fraction of fines passing through each sieve for three different exit plate openings is shown for hematite.

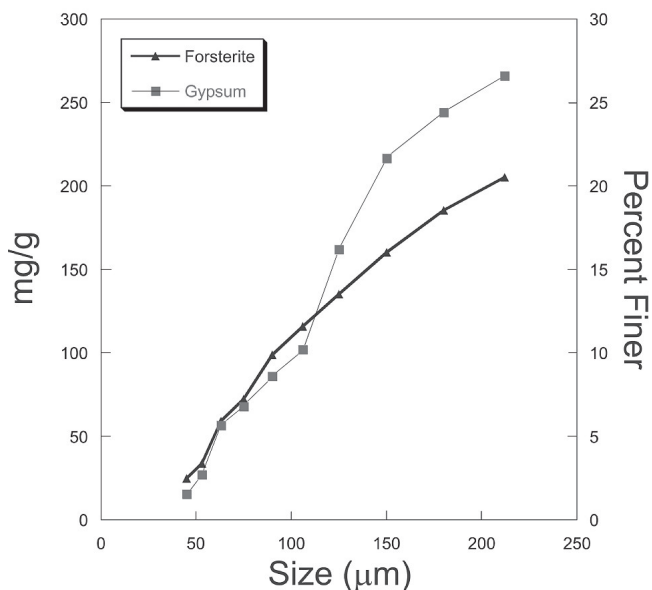


**Figure 10.** Comparison of hard (forsterite) versus soft (gypsum) rock particle size distribution.

diffraction/X-ray fluorescence instrument used to identify the minerals in Mars' rocks and soil. Chemin requires 10 mg of sample powder, with fines <150  $\mu\text{m}$ . The "SAM, Sample Analysis at Mars" instrument suite includes a gas chromatograph mass spectrometer with a tunable laser spectrometer. Rock powder (also <150  $\mu\text{m}$ ) must be delivered to SAM's ovens for heating to release volatiles and detect organic compounds.

## 6. Crusher Products and Performance

### 6.1. Rocks

[34] SPADE has been run with a set of standard igneous and sedimentary rocks that are potential Mars analogs and/or represent good tests of the range of SPADE performance, listed in Table 1. An extensive set of tests explored the particle size distribution produced by the action of the crusher, measured the homogeneity and exposed surface area of the products, and tested performance against rock hardness. Finding limits was a goal. Were there any rocks

that could not be crushed? (There were not.) Production of fines and fragments were characterized as a function of exit plate separation. Representative science data (microscopic images, spectra) from likely inspection instruments was acquired.

#### 6.1.1. Particle Size Distribution

[35] The size distribution of the product was measured for each case. After crushing, the fines and fragments were loaded into a sieve stack (a series of screens in which the size openings become progressively smaller). The stack used during the study utilized 10 individual sieves. The sieve opening sizes were 212, 180, 150, 125, 106, 90, 75, 63, 53, 45  $\mu\text{m}$ , and the pan, which collects all sizes that are small enough to pass through the 45- $\mu\text{m}$  sieve. This size range represents the fine fraction of the particle size distribution. Particles that are too large to fall through to the next screen are considered the "retained material" for that particular screen; materials that are small enough to fall through a screen are noted as "materials passing" or as the "fraction finer" to that screen size.

[36] The mass of each sieve's retained material was recorded and is used to characterize the particle size distribution. Some sets were measured separately to observe homogeneity or to identify specific patterns in the particle size distribution or to examine patterns in the production of newly exposed surfaces.

#### 6.1.2. Exit Plate Configurations

[37] Configuration adjustments were made to the crusher during the course of the study. The gap size at the bottom of the jaw was altered by installing a different thickness fixed plate to test the production of fines versus fragments for a variety of exit gap separations. The three exit gap separations tested were 1.6 mm (0.0625 in.), 3.2 mm (0.125 in.), and 6.3 mm (0.25 in., the original configuration), summarized in Table 2.

[38] Figures 7, 8, and 9 show particle size distributions for the following three possible Martian analogues: forsterite (hard), gypsum (soft), and hematite. In general, the smaller exit slot produced more mass at smaller particulate size, as one would expect. MSL requirements are met in all cases. The smaller the exit slot, the longer it took to crush a rock; typical crushing times were ~2–3 hours. The crushing time varied with the size and the shape of the rock; the more

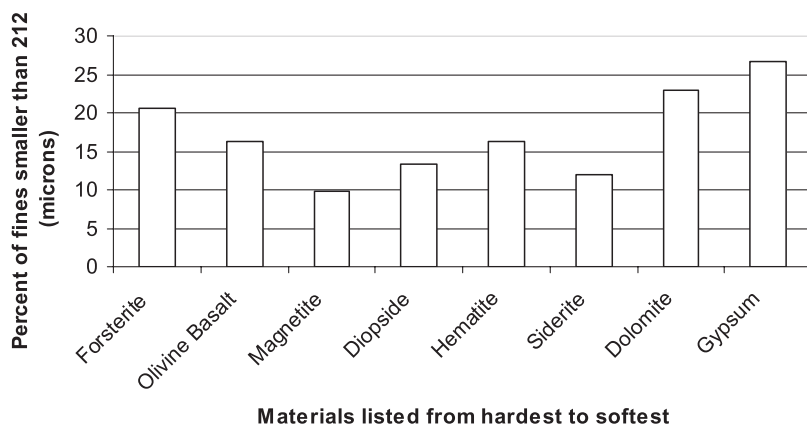


**Figure 11.** Production of fines as a function of mineral hardness.



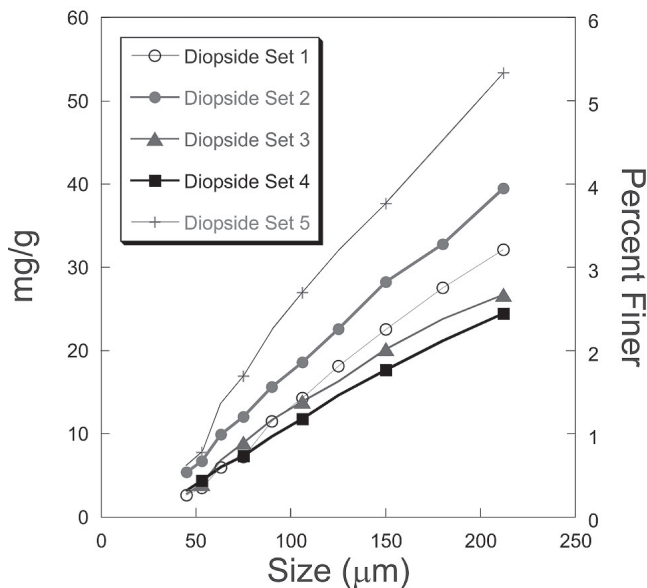


**Figure 12.** Retained diopside crushings utilizing the wide exit configuration, through the crushing process. Set 1 was crushed first, set 2 second, etc. This data illustrates the homogeneity of the crushed particle size distribution throughout the process.

angular the rock, the more pressure points exist for early spallation and fracturing of the sample.

#### 6.1.3. Hardness

[39] Experiments were carried out to address the question of whether rock hardness has an effect on the particle size distribution or the quantity of fines produced. Figure 10 shows the size distribution for the following two extremes: gypsum and forsterite. The results are very similar for fines  $<125\ \mu$ . In Figure 11 the total amount of fines less than  $212\ \mu$  is plotted against rock hardness for a series of minerals. Minerals are listed in order of their hardness, from forsterite (the hardest) to gypsum (the softest), tested in the narrow exit configuration. The amount of fines is not strongly coupled to

the rock hardness. Both sets of data show that the crusher can produce the required amount of fines regardless of sample hardness.

#### 6.1.4. Homogeneity

[40] A carousel with multiple bins enables “splitting” samples of the same rock, sending some of the fines to one instrument and other fines (of the same rock) to another scientific instrument. In this mode of operation, one sample would have been processed earlier in the progression than the other. The next set of tests characterized how well the interior/unweathered portion of the rock is represented throughout the crushing progression.

[41] Figure 12 shows the fines’ size distribution at different times in the crushing cycle (set 1 was crushed first, set 2 second, etc.). All of the diopside crushings smaller than  $180\ \mu$  were retained within 1% of the total regardless of when they were produced in the progression, and all sets show the same general shape. The particle size distribution remained approximately constant from the beginning to the end of the process. Set 5, crushed last, has more fines because, by the end of the crushing process, mostly small rock pieces remained.

[42] There is an inherent limitation to the accuracy with which composition from the fine material can be certain to represent the bulk composition of the rock. If the rock matrix has small hard inclusions, such as a cementing material in a sandstone, then the inclusions may slip through the exit slot without being crushed into fines. To the extent that this happens, the fine composition will not be an exact representation of the bulk rock. This mineral/phase segregation has been documented [Chipera *et al.*, 2004] and is under further investigation. This issue plays into the science instruments that examine the fines; if they are unable to detect mineral phases and elemental composition below some level, any such segregation may not be observed.

#### 6.1.5. Crushing Energy as a Measure of Rock Compressive Strength

[43] The relationship between crushing energy and rock compressive strength has been examined at an exploratory

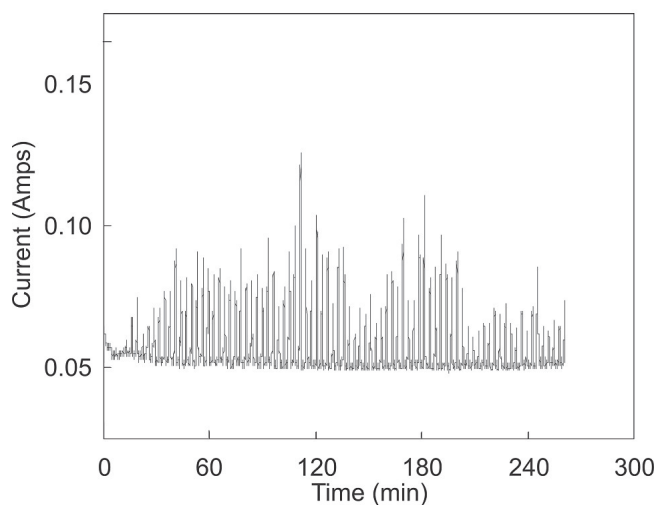


**Figure 13.** Measured crusher motor current for a 35-mm limestone core with a compressive strength of 15 MPa.

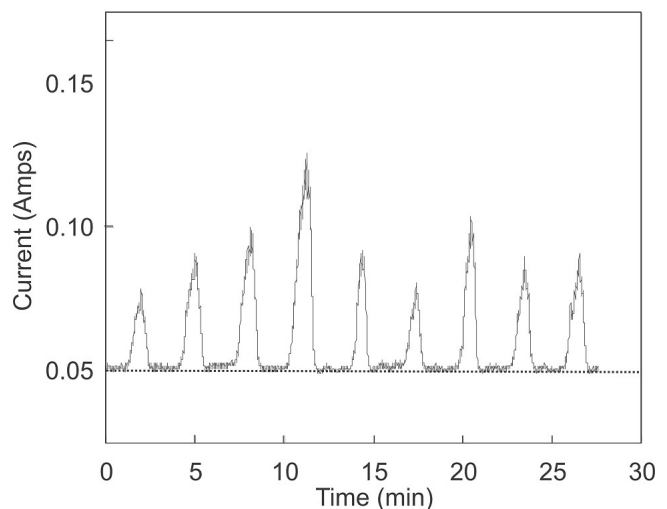


**Figure 14.** Expanded view of the limestone motor current data indicating the baseline current subtracted from the integral used to determine the motor energy associated with crushing.

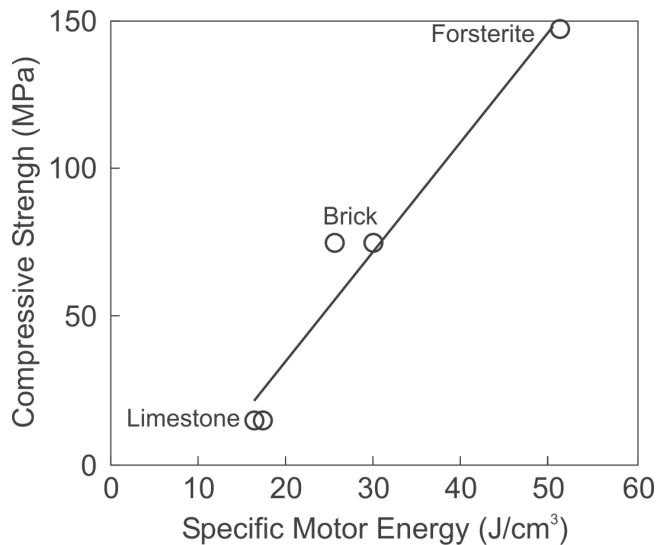


**Figure 15.** Results from crushing cores of three materials with compressive strengths 15, 75, 147 MPa.

level to determine the utility of the rock crusher as a tool for characterizing the bulk strength of Martian rocks. Rock friability, or compressive strength, can vary dramatically from constituent mineral hardness and is often indicative of weathering. Theoretical and experimental studies within the mineral processing field have long focused on the energy of comminution and its relation to material properties. The total energy required to process a sample in the rock crusher can be recorded without modification to the existing device. Preliminary experiments described in this section indicate

that the total crushing energy can provide a measure of rock strength.

[44] The hypothesis that grinding energy is proportional to the new surface created, first postulated by *Rittinger* [1867], has been observed to be roughly accurate for a wide range of brittle materials pulverized by a variety of methods. The proportionality constant can depend on several factors such as the rate at which stress is applied to the particles (for example, by impact) and whether particles are crushed singly or in a bed. It is also linearly dependent on the bulk modulus and yield stress, which are closely related to the compressive strength of the crushed material [Rumpf, 1973]. It is noteworthy that, in industrial grinding operations, only a small fraction ( $\sim 1\text{--}3\%$ ) of the energy applied to the material is accounted for by the creation of fresh powder surface, with the majority winding up as heat due to frictional losses inherent to the fracture process [Harris, 1967]. Using the rock crusher to pulverize a set of materials with known compressive strengths should yield an empirical relationship between applied energy and compressive strength. The assumptions behind this prediction are discussed below.

[45] We assume that the resulting particle size distribution, and hence new surface area, for each material tested is the same with the maximum particle size determined by the crusher gap. We also assume that the energy delivered to the crushed material is a constant fraction of the electrical energy applied to the crusher motor. A variation of this fraction with motor temperature is anticipated and will require calibration. The starting position of the sample in the crusher jaws will also influence the energy required for crushing, although, in the case of cores, the initial height is uniform for all samples. A further assumption made is that crushing energy is proportional to volume and not the mass



a.



b.

**Figure 16.** The Crushed Rock Uniform Dumping Device (CRUDD) was used to measure the potential for cross contamination of samples. (a) The CRUDD in the up (loaded) position. (b) The CRUDD in the down (dump) position.

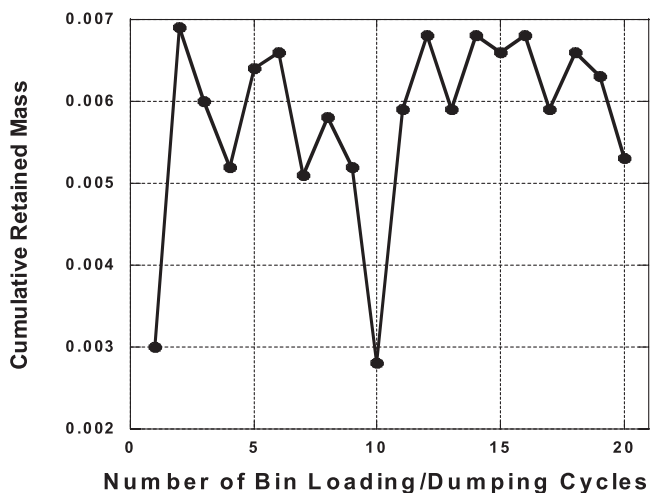


**Figure 17.** This graph illustrates the cumulative set of contamination tests. A clean sample bin was loaded with 10 g of crushed diopside, then discharged using the CRUDD. After recording the leftover mass and without further cleansing, the sample bin was loaded with precisely 10 g again. The loaded material was dumped, and the leftover mass recorded a second time. Twenty tests recorded an average of 0.0058% leftover mass with a standard deviation of 0.0011%.

of crushed material. Specific motor energy is therefore calculated per sample volume derived from the measured rock mass and density.

[46] Two sample cores were crushed from each of the following three materials: forsterite, brick, and limestone. Each cylindrical core measured 22 mm in diameter and 35 mm in length. Compressive strengths for the materials were determined by cutting three 2-in. cubes of each rock and breaking these in a GeoTest S5830 Multiloader Compressive Strength Tester according to ASTM C109/C 109M-02, the standard test method for compressive strength of hydraulic cement mortars. Motor current was monitored at a rate of three samples per second in the 12-volt circuit and integrated

with respect to time to derive the motor energy. The integral of the baseline associated with the bottom of the motor current peaks, which represents the 'rest' power level of the crusher, was subtracted from the total motor energy to isolate the fraction of motor power expended during crushing.

[47] Data from crushing a core of limestone with a compressive strength determined at 15 MPa is illustrated in Figure 13. An expanded view of the motor current and rest level baseline used in the integration is given in Figure 14. Figure 15 is a plot of the specific motor energy versus compressive strength derived from the six tests. These preliminary results suggest that rock compressive strength could be estimated to within 15% by analysis of the calibrated crusher current. Additional tests to demonstrate repeatability and sensitivity to temperature should be carried out to establish the validity of these measurements for the MSL application.

## 6.2. Crusher Products and Performance—Ice

[48] Although the crusher is not designed for crushing ice it is important to understand the behavior of the crusher in the case that a chunk of ice is inadvertently introduced.

[49] A first-order qualitative assessment was carried out. The initial tests used a Mars-analog mixture of clay and ice. The result of introducing this dirty ice into the crusher at  $-20^{\circ}\text{C}$  was pressure melting, and the chunk of ice stuck to the side of the crusher. At  $-80^{\circ}\text{C}$ , the chunk slid up and down the sides of the crusher without getting crushed. Both tests were done at ambient pressure and humidity. The crusher was cooled down before the introduction of the sample into the crusher.

[50] The final test was performed at  $-110^{\circ}\text{C}$ , 6 millibar pressure. In this case a pure water ice chunk was introduced into the crusher. The crusher was able to fragment the ice successfully, however, nearly 6 hours were required.

## 7. Cross-Contamination Investigations

[51] The system was designed to process multiple samples, thus a potential for previously processed samples to contaminate succeeding samples is created. The sample bins

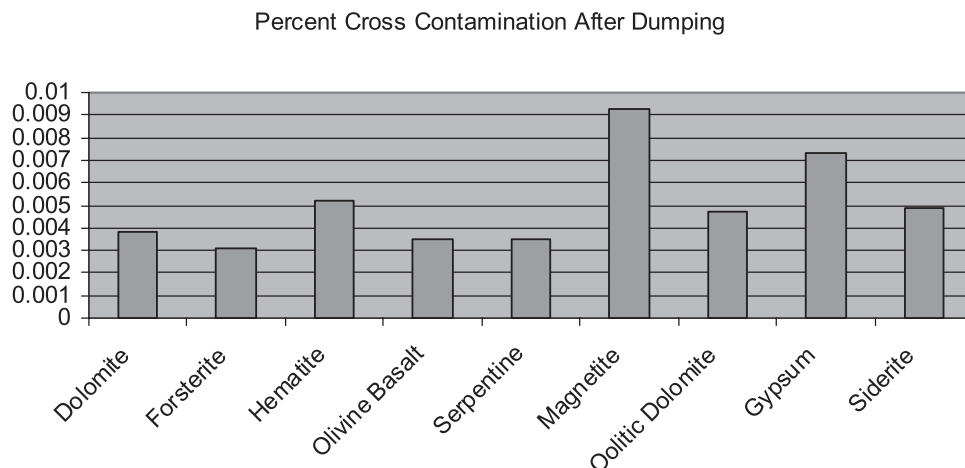


**Figure 18.** Potential cross contamination from one sample to the next is within MSL requirements for all materials tested except magnetite.



are central to the materials transport and delivery system, thus they were the focus of the cross-contamination study. They receive the crushed products directly from the crusher and are used to transport samples that are to be discharged into the front-end systems of in situ instruments. The sample bins may be loaded and discharged many times during the course of a mission.

[52] In order to quantify the cross-contamination potential, it was necessary to measure the mass of the dust that was left on a test bin's surface after processing, handling, and discharging crushed products. Only materials that become transferred from the bin's surface to succeeding samples are considered cross contaminants. For this reason the measured leftover mass is described as the "potential" cross contamination.

[53] The Crushed Rock Uniform Dumping Device (CRUDD) was designed and constructed in order to simulate the trap door operation and to test gravitational bin discharging in a uniform manner. Polished test bins that could be fastened to the CRUDD, as shown in Figure 16, were fabricated. Each test bin was cleaned with alcohol and dried prior to fastening them to the CRUDD. Ten grams  $\pm 10 \mu\text{g}$  of crushed material was loaded onto the test bin. At the triggering of the release lever, the loaded test bin rotated rapidly from a level position to  $90^\circ$  vertical, ending in a "tap" against a solid stop, dumping the material. The uncleaned test bin was then reweighed. The net mass, i.e., the mass of the dusty layer left behind, on the bin surface was recorded.

[54] Figure 17 shows the "cumulative" mass in the bin during the course of 20 sample loadings with just the tap to clean the bins. The measured results are about 2 orders of magnitude less than the amount specified in the MSL Proposal Information Package of 0.5%. Figure 18 tabulates similar experiments for the complete suite of Martian mineral analogs.

[55] Investigations of other methods of cleaning the bins were pursued and reported at the International Conference on Environmental Systems (ICES) [Rohatgi and Shakkottai, 2003]. Rohatgi and Shakkottai focused theoretical calculations on 10- to  $100\text{-}\mu\text{m}$ -size particles held to the sides of the bins by electrostatic forces. They found that a combination of ultrasonic vibration and  $\text{CO}_2$  jets is an effective means of cleaning the bins and preventing cross contamination of the samples.

## 8. Engineering Considerations

[56] From an engineering standpoint, there are a number of techniques available for gaining access to the interiors of rocks. The SPADE approach of fragmenting rocks in a crusher has the following advantages:

[57] • **Demonstrated capability.** Rock crushers are simple and robust devices that have been used in ore processing for hundreds of years.

[58] • **Self-contained process.** Once a rock has been placed in a crusher, the remaining processes are self-contained. Using a rock crusher on a rover (1) does not require the rover to resolve and react to directional forces exerted against fixed or moveable samples and (2) is not affected by the positioning accuracy of the rover relative to the rock or the stability of the rover. Recall that the forces required to crush rocks on Mars are the same as those on Earth, but the

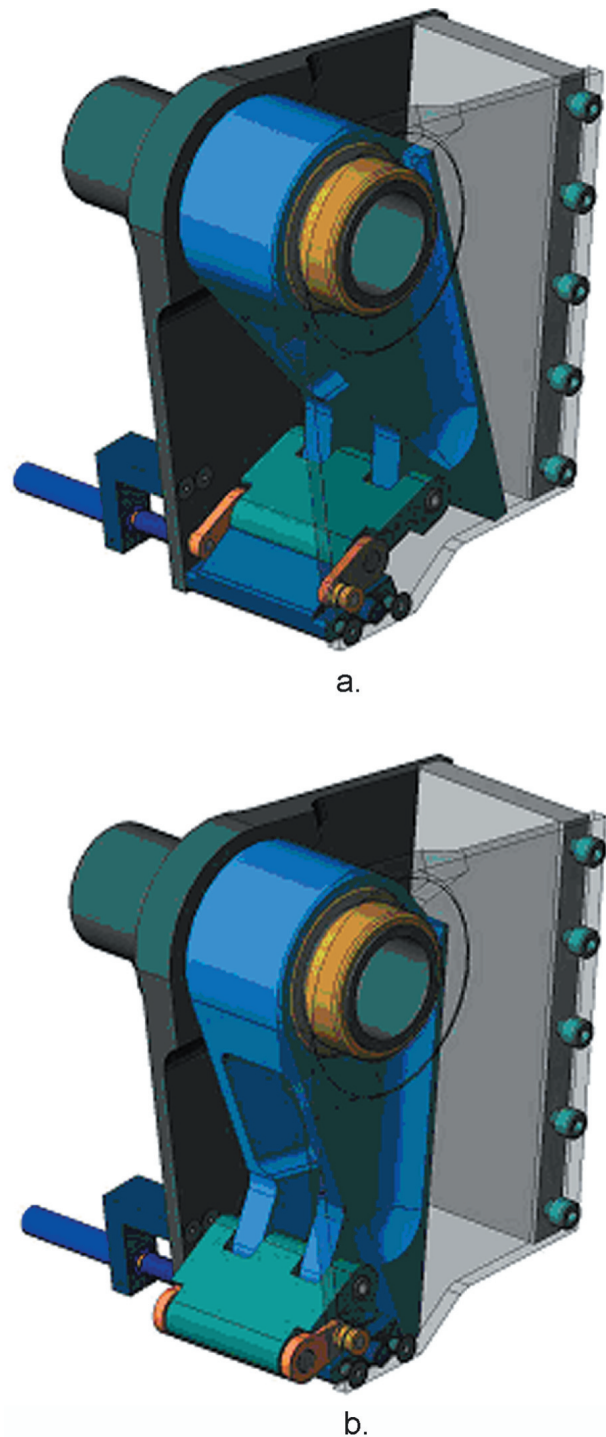


**Figure 19.** (a) The "snake jaw" rock release mechanism is shown in the closed position and (b) in the open position.

gravitational forces that hold rocks and rovers in place on Mars are only 1/3 of those on Earth.

[59] • **Low power requirements.** The rock crusher requires less than 6 W to crush any rock.

[60] • **Operational simplicity.** Rock crushing is a simple, gravity-fed, low vibration, repetitive process that, once initiated, can be carried to completion in an autonomous manner.

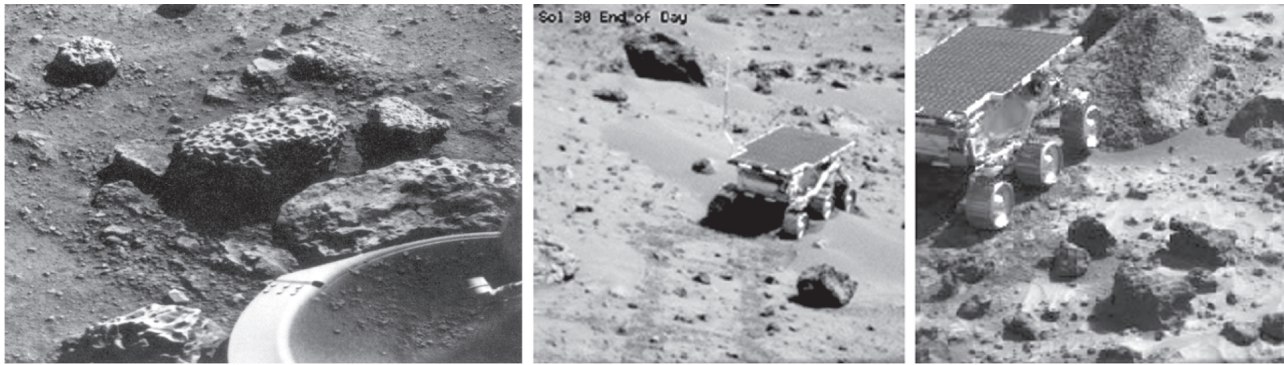


**Figure 20.** Mars surface images. Viking Lander 2 (left) and Pathfinder (center and right) images illustrate the presence of abundant rocks in the 5-cm size range on the Martian surface. For scale, the Pathfinder Rover's wheels are approximately 12 cm in diameter.

[61] • Reusability. Rock crushers require no consumable or replaceable parts and thus place no limits on the number of samples that can be investigated within the lifetime of the rover.

## 9. Fault Tolerance

[62] There may be times when it is desirable to release a rock before it has been crushed to completion. For example, large fresh rock faces may be best for characterization by a remote investigation instrument, or it may be determined part way through the crush process that the rock is similar to previous samples and it is not necessary to crush to completion. Although the rock crusher has successfully crushed our test rocks, it is also conceivable that a rock may prove impossible to crush.

[63] A mechanism termed the “snake jaw” has been designed to open the bottom of the crusher and release a rock any time during the crushing process. In its open position the plates are parallel and the width at the bottom is equal to the top. The snake jaw uses an articulating brace that is locked in position during the crush process. Open and closed positions are shown in Figure 19. The snake jaw provides a robust recovery in the event of a jammed sample.

## 10. Constraints on Functionality

[64] The major constraint on the functionality of the SPADE is that the shape and size of a rock acquired for analysis must be suitable for crushing. After considering a number of factors, including the mass and volume available for the crusher, the forces required to crush rocks, and the capabilities of the robotic arm, the ‘01 Rockhound team concluded that the baseline design for the Rockhound crusher should be capable of accepting rocks up to approximately 5-cm diameter. A 5-cm rock diameter is adequate to insure the inclusion of pristine interior material even with a weathered rind up to 2 cm thick all around. The crusher can be designed for larger rocks, with correspondingly greater mass and volume.

[65] The scientific limitations of sampling rocks in the 5-cm size range are not expected to be severe. The Viking, Pathfinder, and Spirit landers and rovers found their landing sites to be littered with rocks in this size range, as illustrated in Figure 20 for Viking and Pathfinder. At the Viking sites,

the number density of 5-cm rocks was approximately 30 times that of 50-cm rocks [Moore *et al.*, 1987]. If anything, these statistics suggest that a system designed to sample smaller rocks will have many more potential targets than the one designed to sample only larger rocks. Obviously, if no rocks in the desired size range are available, then the rover's mobility can be put to use to find a more suitable sampling area. Thus far, there has been no evidence suggesting that the properties of the smaller rocks at the Viking, Pathfinder, and Spirit landing sites differ from those of the larger ones. Since 5-cm rocks would not be expected to be transported for great distances by Martian winds, there is no reason to expect that rocks in this size range would be any less representative of the local geology than the larger rocks.

## 11. Conclusion

[66] The SPADE system is a viable means for accessing the interior of rocks on Mars, as a component of a payload on a landed or roving mission on the surface of Mars. Resource requirements such as mass, power, and volume are well within the capacities of such a mission. The potential scientific payoff, the opportunity to decipher the geologic and climate history of Mars by means of studying its rocks, is immeasurable.

[67] **Acknowledgments.** Valuable contributions to the original design were made by Tim Ohm. J. Anthony Smith provided substantial support for the production of the figures. This work was partially performed at the Jet Propulsion Laboratory, California Institute of Technology, under a contract with the National Aeronautics and Space Administration.

## References

- Arvidson, R. E., J. L. Gooding, and H. J. Moore (1989), The Martian surface as imaged, sampled, and analyzed by the Viking landers, *Rev. Geophys.*, 27, 39–60.
- Baker, V. R. (2001), Water and the Martian landscape, *Nature*, 412, 228–236.
- Bandfield, J. L., V. E. Hamilton, and P. R. Christensen (2000), A global view of Martian surface compositions from MGS-TES, *Science*, 287, 1626–1630.
- Bell, J. F., III, et al. (2000), Mineralogic and compositional properties of Martian soil and dust: Results from Mars Pathfinder, *J. Geophys. Res.*, 105, 1721–1756.
- Bell, J. F., III, et al. (2004), Pancam multispectral imaging results from the Spirit rover at Gusev Crater, *Science*, 305, 800–806.
- Biemann, K., et al. (1977), The search for organic substances and inorganic volatile compounds in the surface of Mars, *J. Geophys. Res.*, 82, 4641–4658.

- Boynton, W. V., et al. (2002), Distribution of hydrogen in the near surface of Mars: Evidence for subsurface ice deposits, *Science*, 296, 81–85.
- Carr, Michael H. (1981), *The Surface of Mars*, Yale Univ. Press, New Haven.
- Chipera, S. J., D. T. Vaniman, D. L. Bish, P. Sarrazin, S. Feldman, D. F. Blake, G. Bearman, and Y. Bar-Cohen (2004), Evaluation of rock powdering methods to obtain fine-grained samples for CHEMIN, a combined XRD/XRF instrument, paper presented at Lunar and Planetary Science Conference XXXV, Lunar and Planetary Institute, League City, TX.
- Christensen, P. R., and S. W. Ruff (2004), Formation of the hematite-bearing unit in Meridiani Planum: Evidence for deposition in standing water, *J. Geophys. Res.*, 109, E08003, doi:10.1029/2003JE002233.
- Christensen, P. R., J. L. Bandfield, M. D. Smith, V. E. Hamilton, and R. N. Clark (2000), Identification of a basaltic component on the Martian surface from Thermal Emission Spectrometer data, *J. Geophys. Res.*, 105, 9609–9621.
- Christensen, P. R., R. V. Morris, M. D. Lane, J. L. Bandfield, and M. C. Malin (2001), Global mapping of Martian hematite mineral deposits: Remnants of water-driven processes on early Mars, *J. Geophys. Res.*, 106, 23,873–23,885.
- Christensen, P. R., et al. (2004), Initial results from the Mini-TES experiment in Gusev Crater from the Spirit rover, *Science*, 305, 835–841.
- Gellert, R., et al. (2004), Chemistry of rocks and soils in Gusev Crater from the Alpha Particle X-ray Spectrometer, *Science*, 305, 829–832.
- Gooding, J. L., R. E. Arvidson, and M. Y. Zolotov (1992), Physical and chemical weathering, in *Mars*, edited by H. H. Kieffer, B. M. Jakosky, C. W. Snyder, and M. S. Matthews, pp. 686–729, Univ. of Ariz. Press, Tucson, AZ.
- Hansen, C. J., D. A. Paige, and P. Smith (1997), Rockhound: An integrated payload for the Mars Surveyor Program 2001 rover, Proposal in response to NASA Announcement of Opportunity AO 97-OSS-04.
- Hansen, C. J., D. A. Paige, and W. Zimmerman (2001), RockSys: A rock crusher and sample sorting and distribution system designed for a Mars rover, PIDDP Proposal 00-OSS-01 PID 344-36-20-45A.
- Harris, C. C. (1967), On the role of energy in comminution: A review of physical and mathematical principles, *Trans. SME*, 75, 37–56.
- Herkenhoff, K. E., et al. (2004), Textures of the soils and rocks at Gusev Crater from Spirit's microscopic imager, *Science*, 305, 824–826.
- Hoefen, T. M., R. N. Clark, J. L. Bandfield, M. D. Smith, J. C. Pearl, and P. R. Christensen (2003), Discovery of olivine in the Nili Fossae region of Mars, *Science*, 302, 627–630.
- Johnson, J. R., P. R. Christensen, and P. G. Lucey (2002), Dust coatings on basaltic rocks and implications for thermal infrared spectroscopy of Mars, *J. Geophys. Res.*, 107(E6), 5035, doi:10.1029/2000JE001405.
- Malin, M. C., and K. S. Edgett (2003), Evidence for persistent flow and aqueous sedimentation on early Mars, *Science*, 302, 1931–1934.
- McSween, H. Y., et al. (1999), Chemical, multispectral and textural constraints on the composition and origin of rocks at the Mars Pathfinder landing site, *J. Geophys. Res.*, 104, 8679–8715.
- McSween, H. Y., et al. (2004), Basaltic rocks analyzed by the Spirit rover in Gusev Crater, *Science*, 305, 842–845.
- Moore, H. J., R. E. Hutton, G. D. Clow, and C. R. Spitzer (1987), Physical properties of surface materials at the Viking landing sites on Mars, U.S. Geol. Surv. Prof. Pap., 1389.
- Morris, R. V., et al. (2004), Mineralogy at Gusev Crater from the Mossbauer spectrometer on the Spirit rover, *Science*, 305, 833–836.
- Mustard, J. F., and J. M. Sunshine (1995), Seeing through the dust: Martian crustal heterogeneity and links to the SNC meteorites, *Science*, 267, 1623–1626.
- Parker, T. J., D. S. Gorsline, R. S. Saunders, D. C. Pieri, and D. M. Schneeberger (1993), Coastal geomorphology of the Martian northern plains, *J. Geophys. Res.*, 98(E6), 11,061–11,078, doi:10.1029/93JE00618.
- Rittinger, P. R. (1867), *Lehrbuch der Aufbereitungskunde*, Berlin.
- Rohatgi, N., and P. Shakkottai (2003), Cross contamination of Martian rock samples, SAE International Paper 2003-01-2673, presented at 33rd International Conference on Environmental Systems, Vancouver, BC, 7–10 July.
- Rumpf, H. (1973), Physical aspects of comminution and a new formulation of a law of comminution, *Powder Technol.*, 7, 145–159.
- Smith, P. H., et al. (1997), Results from the Mars Pathfinder camera, *Science*, 278, 1758–1765.
- Smith, M. D., J. L. Bandfield, and P. R. Christensen (2000), Separation of atmospheric and surface spectral features in Mars Global Surveyor Thermal Emission Spectrometer (TES) spectra, *J. Geophys. Res.*, 105, 9589–9608.
- Squyres, S. W., et al. (2004a), The Spirit rover's Athena science investigation at Gusev Crater, Mars, *Science*, 305, 794–799.
- Squyres, S. W., et al. (2004b), The Opportunity rover's Athena science investigation at Meridiani Planum, Mars, *Science*, 306, 1698–1703.
- Squyres, S. W., et al. (2004c), In situ evidence for an ancient aqueous environment at Meridiani Planum, Mars, *Science*, 306, 1709–1722.

G. Bearman, S. Fuerstenau,\* C. J. Hansen, J. Horn, C. Mahoney, S. Patrick, G. Peters, J. Scherbenski, L. Shiraishi, and W. Zimmerman, Jet Propulsion Laboratory, California Institute of Technology, 4800 Oak Grove Dr., Pasadena, CA 91109-8099, USA. (candice.j.hansen@jpl.nasa.gov)  
 D. A. Paige, Department of Earth and Space Sciences, UCLA, Los Angeles, CA 90024, USA. (dap@mars.ucla.edu)

\*The author's name is correct here, The article as originally published is online.